Inorg. Chem. **2003**, *42*, 7683–7690

A Family of Diruthenium Compounds with Dianionic Tridentate Ligands of *N*-(2-Pyridyl)-2-oxy-5-R-benzylaminate (R = H, Me, Cl, Br, NO_2): Isolation, Structure Determination, and Electrochemistry

Hitoshi Miyasaka,* Toru Izawa, Ken-ichi Sugiura, and Masahiro Yamashita

Department of Chemistry, Graduate School of Science, Tokyo Metropolitan University, 1-1 Minamiohsawa, Hachioji, Tokyo 192-03, Japan

Received June 6, 2003

The ligand substitution reaction of $Ru_2(O_2CCH_3)_4Cl$ with 5-substituted *N*-(2-pyridyl)-2-oxy-5-R-benzylaminate (R = H, Me, Cl, Br, NO_2) resulted in a family of anionic diruthenium species of $[Ru_2(O_2CCH_3)_2(R\text{-salpy})_2]^-$ that were isolated by using Na^+- or K^+-18-crown-6-ether as the countercation: $[A(18\text{-crown-6})(S)_x][Ru_2(O_2CCH_3)_2(R\text{-salpy})_2]$ (A = Na^+, K^+; S = solvent; R = H, **1**; Me, **2**; Cl, **3**; Br, **4**; NO_2, **5**). All compounds were structurally characterized by X-ray crystallography. The structural features of the anionic parts are very similar among the compounds: two acetate and two R-salpy^{2-} ligands are, respectively, located around the Ru_2 unit in a *trans* fashion, where the R-salpy^{2-} ligand acts as a tridentate ligand having both bridging and chelating characters to form the M–M bridging/axial-chelating mode. Compounds **1** and **5** with K^+-18-crown-6-ether have one-dimensional chain structures, the K^+-18-crown-6-ether interacting with phenolate oxygens of the $[Ru_2(O_2CCH_3)_2(R\text{-salpy})_2]^-$ unit to form a repeating unit, [···K···O–Ru–Ru–O···], whereas **2**–**4** are discrete. Cyclic voltammetry and differential pulse voltammetry revealed systematic redox activities based on the dimetal center and the substituted ligand, obeying the Hammett law with the reaction constants per substituent, ρ, for the redox processes being 127 mV for Ru_2^{5+}/Ru_2^{4+}, 185 mV for Ru_2^{6+}/Ru_2^{5+}, 92 mV for Ru_2^{7+}/Ru_2^{6+}, and 179 mV for R-salpy$^-$/R-salpy^{2-}. For **3**, the singly oxidized and reduced species, Ru_2^{6+} and Ru_2^{4+}, respectively, generated by bulk controlled-potential electrolyses were finally monitored by spectroscopy. The singly oxidized species can also be slowly generated by air oxidation.

Introduction

The development of multi-redox molecular systems is one of the recent themes of intensive research in the field of metal−metal bond chemistry. In the fabrication of target molecules, the introduction of redox-active ligands into a metal−metal bonding core is an exciting synthetic strategy because the obtained materials are expected to undergo redox on both dimetal and ligand centers in one molecule and to exhibit metal−ligand (d−π) electron-conjugated redox behavior.[1−6] As a favorite example of the proposed molecules, Dunbar and co-workers reported a homologous series, $[M_2(O_2CCH_3)_2(pynp)_2]^{2+}$ (M = Mo, Ru, and Rh; pynp = 2-(2-pyridyl)-1,8-naphthridene), the pynp of which is redox-active, and the compounds underwent not only metal-centered redox but also ligand (pynp)-centered redox that was fully electrically coupled between pynp ligands via the M−M unit.[6] Recently, we prepared a new class of N−N−O tridentate ligands for bridging a metal−metal bonding unit denoted by R-salpy^{2-} (*N*-(2-pyridyl)-2-oxy-5-R-benzylaminate).[7] One interesting aspect of this class of ligands is that the phenolate moiety in the R-salpy^{2-} ligand may be electrochemically oxidized even in their dimetal compounds. Therefore, we attempted to synthesize a series of diruthenium compounds with R-salpy^{2-} analogues in order to investigate their redox properties in relation to the R substituents and

* To whom correspondence should be addressed. E-mail: miyasaka@comp.metro-u.ac.jp. Fax: +81-426-77-2525.

(1) Tikkanen, W. R.; Binamira-Soriaga, E.; Kaska, W. C.; Ford, P. *Inorg. Chem.* **1984**, *23*, 141.
(2) Baker, A. T.; Tikkanen, W. R.; Kaska, W. C.; Ford, P. *Inorg. Chem.* **1984**, *23*, 3254.
(3) Bear, L.; Li, Y.; Han, B.; Caemelbecke, E. V.; Kadish, K. M. *Inorg. Chem.* **2001**, *40*, 182.
(4) Bear, L.; Li, Y.; Han, B.; Caemelbecke, E. V.; Kadish, K. M. *Inorg. Chem.* **1996**, *35*, 3053.
(5) Ren, T.; DeSilva, V.; Zou, G.; Lin, C.; Daniels, L. M.; Campana, C. F.; Alvarez, J. C. *Inorg. Chem. Commun.* **1999**, *2*, 301.
(6) (a) Campos-Fernández, C. S.; Ouyang, X.; Dunbar, K. R. *Inorg. Chem.* **2000**, *39*, 2432. (b) Campos-Fernández, C. S.; Thomson, L. M.; Galán-Mascarós, J. R.; Ouyang, X.; Dunbar, K. R. *Inorg. Chem.* **2002**, *41*, 1523.
(7) Miyasaka, H.; Kachi-Terajima, C.; Ishii, T.; Yamashita, M. *J. Chem. Soc., Dalton Trans.* **2001**, 1929.

10.1021/ic034625k CCC: $25.00
Published on Web 10/22/2003

were able to successfully isolate crystal samples of the family by using alkaline metal complexes (Na^+ and K^+) with 18-crown-6-ether as the countercation. In this paper, the isolation, structure determination, and redox chemistry of the following family of diruthenium compounds containing two R-salpy^{2-} ligands are reported: $[A(18\text{-crown-6})(S)_x][Ru_2(O_2CCH_3)_2(R\text{-salpy})_2]\cdot n(\text{solvent})$ (18-crown-6 = 18-crown-6-ether; R = H, **1**, A = K^+; Me, **2**, A = Na^+, S = THF, H_2O; Cl, **3**, A = Na^+, S = THF, H_2O; Br, **4**, A = Na^+, S = THF, H_2O; NO_2, **5**, A = K^+), which undergoes multi-redox on both the diruthenium center and the R-salpy^{2-} ligand. The individual redox potentials show the electronic effect of the introduced ligand on the Hammett law and indicate the ability of the R substituent to tune the redox potentials of the diruthenium unit.

Experimental Section

Materials and Reagents. Syntheses of the diruthenium compounds were carried out under dry nitrogen atmosphere. All chemicals used for the syntheses were of reagent grade. The diruthenium(II,III) compound $Ru_2(O_2CCH_3)_4Cl$ was synthesized according to the method in the literature.[8] R-salpy^{2-} ligands were synthesized by the chemical reduction of the corresponding Schiff base precursors using $NaBH_4$ in methanol, and finally characterized by ^1H NMR, elemental analysis, and IR spectroscopy. All solvents used for the syntheses of the Ru_2 compounds as well as for electrochemical and spectroscopic studies were dried by refluxing over conventional drying agents and freshly distilled under nitrogen atmosphere before use.

Preparation of Diruthenium Compounds. A methanol solution (15 cm^3) of salpyH_2 (120 mg, 0.6 mmol) for **1**, 5-MesalpyH_2 (128 mg, 0.6 mmol) for **2**, 5-ClsalpyH_2 (141 mg, 0.6 mmol) for **3**, 5-BrsalpyH_2 (167 mg, 0.6 mmol) for **4**, or 5-NO_2salpyH_2 (147 mg, 0.6 mmol) for **5** containing NaOH (48 mg, 1.2 mmol) for **2**, **3**, and **4**, or KOH (67 mg, 1.2 mmol) for **1** and **5**, was added to a solid of $Ru_2(O_2CCH_3)_4Cl$ (142 mg, 0.3 mmol), and the brown suspension was stirred overnight at room temperature. During this time, the brown suspension was gradually transformed into a dark green solution with some precipitates. Then, the solution was filtered to remove insoluble solids, and the filtrate was evaporated under reduced pressure. The green solid was dissolved again in 18 cm^3 of THF containing 18-crown-6-ether (317 mg, 1.2 mmol), and the obtained solution was then stirred for 10 min at room temperature. The filtered solution was pipetted into a narrow Schlenk tube for diffusion with 18 cm^3 of toluene to form rectangular green crystals.

[K(18-crown-6)][Ru$_2$(O$_2$CCH$_3$)$_2$(salpy)$_2$]·0.5THF (1·0.5THF). Yield: 42 mg, 13%. Anal. Calcd for $C_{42}H_{54}KN_4O_{12.5}Ru_2$: C, 47.76; H, 5.15; N, 5.30. Found: C, 47.76; H, 5.11; N, 5.31. IR (KBr, cm^{-1}): 3423 (m), 2897 (m), 1603 (m), 1589 (m), 1472 (s), 1448 (s), 1433 (s), 1352 (m), 1286 (m), 1107 (s), 961 (m), 754 (m). UV−vis (λ_{max}/nm (10^{-3} ϵ/M^{-1}·cm^{-1}) in MeCN): 430 (sh), 581 (2.8), 680 (sh), 1046 (0.8).

[Na(18-crown-6)(OC$_4$H$_8$)(H$_2$O)][Ru$_2$(O$_2$CCH$_3$)$_2$(5-Mesalpy)$_2$]·0.5H$_2$O (2·0.5H$_2$O). Yield: 38 mg, 11%. Anal. Calcd for $C_{46}H_{65}N_4NaO_{14.5}Ru_2$: C, 48.84; H, 5.75; N, 4.95. Found: C, 48.98; H, 5.68, N, 4.95. IR (KBr, cm^{-1}): 3410 (w, br), 2897 (w), 1603 (m), 1481 (s), 1467 (s), 1431 (m), 1352 (m), 1283 (s), 1190 (s), 962 (w), 837 (w), 758 (w). UV−vis (λ_{max}/nm (10^{-3} ϵ/M^{-1}·cm^{-1}) in MeCN): 308 (22), 442 (5.6), 582 (5.1), 680 (sh), 1045 (1.3).

[Na(18-crown-6)(THF)(H$_2$O)][Ru$_2$(O$_2$CCH$_3$)$_2$(5-Clsalpy)$_2$] (3). Yield: 76 mg, 22%. Anal. Calcd for $C_{44}H_{58}Cl_2N_4NaO_{14}Ru_2$: C, 45.43; H, 5.03; N, 4.82. Found: C, 45.24; H, 4.83; N, 4.93. IR (KBr, cm^{-1}): 3414 (br, m), 2909 (w), 1603 (m), 1466 (s), 1433 (s), 1285 (m), 1109 (s), 962 (w), 839 (w), 760 (w), 662 (w). UV−vis (λ_{max}/nm (10^{-3} ϵ/M^{-1}·cm^{-1}) in MeCN): 312 (sh), 438 (5.2), 585 (5.1), 670 (sh), 1046 (1.6).

[Na(18-crown-6)(THF)(H$_2$O)][Ru$_2$(O$_2$CCH$_3$)$_2$(5-Brsalpy)$_2$] (4). Yield: 154 mg, 41%. Anal. Calcd for $C_{44}H_{58}Br_2N_4NaO_{14}Ru_2$: C, 42.21; H, 4.67; N, 4.47. Found: C, 42.30; H, 4.68; N, 4.60. IR (KBr, cm^{-1}): 3423 (br, w), 2901 (w), 1602 (m), 1466 (m), 1433 (m), 1352 (w), 1285 (m), 1107 (m), 961 (w), 839 (w), 758(w). UV−vis (λ_{max}/nm (10^{-3} ϵ/M^{-1}·cm^{-1}) in MeCN): 290 (sh), 437 (5.3), 584 (4.4), 670 (sh), 1051 (1.3).

[K(18-crown-6)][Ru$_2$(O$_2$CCH$_3$)$_2$(5-NO$_2$salpy)$_2$] (5). Yield: 86 mg, 26%. Anal. Calcd for $C_{40}H_{48}KN_6O_{16}Ru_2$: C, 43.27; H, 4.36; N, 7.57. Found: C, 43.47; H, 4.38; N, 7.70. IR (KBr, cm^{-1}): 2901 (w), 1603 (m), 1587 (m), 1489 (m), 1468 (m), 1435 (m), 1281 (s), 1165 (m), 1105 (m), 961 (w), 764 (w). UV−vis (λ_{max}/nm (10^{-3} ϵ/M^{-1}·cm^{-1}) in MeCN): 580 (sh), 640 (sh), 1043 (0.7).

Physical Measurements. Infrared spectra were measured on KBr disks with a Shimadzu FT-IR 8600 spectrophotometer. General magnetic susceptibility data for ground samples were measured over the temperature range 1.8−300 K using an MPMS-XL SQUID susceptometer (Quantum Design, Inc.), where the applied magnetic fields were 1 T. Corrections were made for diamagnetism using Pascal's constants[9] and for vinyl capsule wrapping samples. The UV−vis−NIR spectrum was measured in degassed acetonitrile (MeCN) in a septum-sealed cell using a Hitachi U-3500 spectrophotometer. Cyclic voltammograms (CVs) and differential-pulse voltammograms (DPVs) were recorded in MeCN (*n*-tetrabutylammonium tetrafluoroborate [TBA(BF$_4$)] = 0.2 M as a supporting electrolyte) under a nitrogen atmosphere with the use of an ALS/CHI Instruments electrochemical analyzer (model CHI 600A). At the beginning of measurement of the compounds, the CVs of acetonitrile with only supporting electrolyte were measured. To this solution were added the compounds ([compound] = 2×10^{-4} M), and the resultant solution was measured with a unit of carbon working electrode, Pt counter electrode, and Ag/AgCl reference electrode. Finally, CV potentials were justified by using the ferrocene/ferrocenium couple as an internal reference (Fc/Fc^+ = 0.08 V (ΔE = 75 mV) in MeCN vs Ag/AgCl). Bulk controlled-potential electrolyses were carried out for **3** using the same apparatus in MeCN solutions containing 0.2 M of **3** and TBA(BF$_4$) under N_2 at potentials slightly more positive than $E_{1/2}^{((1-e)ox)}$ and slightly more negative than $E_{1/2}^{((1-e)red)}$. The passage and completion of electrolyses were monitored from conducting current.

X-ray Crystallographic Analyses. Measurements were conducted on a Rigaku Raxis-Rapid imaging plate diffractometer with graphite monochromated Mo Kα radiation (λ = 0.71069 Å). The data were collected up to 55°. The structures were solved by direct methods (SIR92)[10] and expanded using Fourier techniques.[11] Non-hydrogen atoms were refined anisotropically, whereas hydrogen atoms were introduced as fixed contributors. For full-matrix least-squares refinements based on the $I > 2.00\sigma(I)$ or $I > 3.00\sigma(I)$

(8) Mitchell, R. W.; Spencer, A.; Wilkinson, G. *J. Chem. Soc., Dalton Trans.* **1972**, 846.

(9) Boudreaux, E. A.; Mulay, L. N. *Theory and Applications of Molecular Paramagnetism*; John Wiley and Sons: New York, 1976; pp 491−495.

(10) Altomare, A.; Burla, M. C.; Camalli, M.; Cascarano, M.; Giacovazzo, C.; Guagliardi, A.; Polidori, G. *J. Appl. Crystallogr.* **1994**, *27*, 435.

(11) Beurskens, P. T.; Admiraal, G.; Beurskens, G.; Bosman, W. P.; de Gelder, R.; Israel, R.; Smits, J. M. M. *The DIRDIF program system*; Technical Report of the Crystallography Laboratory; University of Nijmegen: Nijmegen, The Netherlands, 1994.

Table 1. Crystallographic Data of **1**−**5**

	1·toluene	**2**·0.5THF	**3**·0.5THF	**4**·0.5THF	**5**·2toluene
empirical formula	$C_{47}H_{58}N_4O_{12}KRu_2$	$C_{48}H_{68}N_4O_{14.5}NaRu_2$	$C_{46}H_{64}N_4O_{14.5}Cl_2NaRu_2$	$C_{46}H_{64}N_4O_{14.5}Br_2NaRu_2$	$C_{54}H_{60}N_6O_{16}KRu_2$
fw/g·mol^{-1}	1112.23	1158.21	1201.07	1289.97	1290.34
space group	$P\bar{1}$ (No. 2)	$C2/c$ (No. 15)	$C2/c$ (No. 15)	$C2/c$ (No. 15)	$P\bar{1}$ (No. 2)
T/°C	−150(1)	−150(1)	−150(1)	−150(1)	−170(1)
λ/Å	0.71069	0.71069	0.71069	0.71069	0.71069
a/Å	8.7174(4)	18.2978(7)	18.2519(6)	18.1722(3)	8.774(4)
b/Å	11.538(2)	16.8318(5)	16.8349(5)	16.8797(2)	12.977(6)
c/Å	12.790(2)	33.878(1)	33.904(1)	34.4686(4)	14.017(4)
α/deg	84.31(1)	90	90	90	112.59(2)
β/deg	70.65(2)	99.499(2)	99.167(2)	100.0737(4)	96.74(2)
γ/deg	79.860(9)	90	90	90	107.81(1)
V/Å^3	1193.5(3)	10290.9(6)	10284.7(6)	10409.9(2)	1351.8(10)
Z	1	8	8	8	1
D_{calcd}/g·cm^{-3}	1.547	1.495	1.551	1.646	1.585
μ(Mo Kα)/cm^{-1}	0.786	0.664	0.768	2.196	0.712
unique reflns	3947 ($I > 3.00\sigma(I)$)	7489 ($I > 3.00\sigma(I)$)	7590 ($I > 3.00\sigma(I)$)	6380 ($I > 3.00\sigma(I)$)	4958 ($I > 2.00\sigma(I)$)
no. variables	313	627	627	627	358
GOF	1.128	1.144	1.142	1.329	1.209
R1[a]	0.0860 ($I > 3.00\sigma(I)$)	0.0548 ($I > 3.00\sigma(I)$)	0.0773 ($I > 3.00\sigma(I)$)	0.0411 ($I > 3.00\sigma(I)$)	0.0496 ($I > 2.00\sigma(I)$)
wR2[b,c]	0.2332 (all data)	0.1596 (all data)	0.2348 (all data)	0.0993 (all data)	0.1619 (all data)

[a] $R1 = \sum||F_o| - |F_c||/\sum|F_o|$. [b] $wR2 = [\sum w(F_o^2 - F_c^2)^2/\sum w(F_o^2)^2]^{1/2}$. [c] $w = 1/[\sigma^2F_o^2 + (p(\max(F_o^2,0) + 2F_c^2)/3)^2]$ for **1**, where $p = 0.200$ for **1**, 0.122 for **2**, 0.200 for **3**, 0.049 for **4**, and $w = 1/[\sigma^2F_o^2 + (0.1P)^2]$, where $P = (F_o^2 + 2F_c^2)/3$ for **5**.

reflections and observed reflections, the unweighted and weighted agreement factors of $R1 = \sum||F_o| - |F_c||/\sum|F_o|$ (σ-cut data), and $wR2 = [\sum w(F_o^2 - F_c^2)^2/\sum w(F_o)^2]^{1/2}$ (all data), were used. All calculations were performed using the teXsan crystallographic software package of Molecular Structure Corporation.[12] Crystal data and details of the structure determination of **1**−**5** are summarized in Table 1.

Results and Discussion

Syntheses and Characterization. The family of diruthenium compounds was prepared using an identical synthetic procedure: the reaction of $Ru_2(O_2CCH_3)_4Cl$ with R-salpyH_2 (1:2) in a methanolic medium in the presence of a deprotonating reagent, NaOH or KOH, gave a brown solution containing $[Ru_2(O_2CCH_3)_2(R\text{-salpy})_2]^-$. The ligand substitution reaction in a 1:2 ratio thus resulted in a stoichiometric product. We also attempted a similar reaction in a 1:3 ratio using 5-Clsalpy^{2-}, which resulted in a 1:3 product, $[Li_2(THF)_4Cl\{Ru_2(5\text{-Clsalpy})_3\}]$, as expected.[13] The crown-ether complexes of alkaline-metal ions sometimes act as good cations for the crystallization and isolation of anionic species.[14] In a similar manner, the addition of 18-crown-6-ether to form a Na^+- or K^+-18-crown-6-ether cationic complex led to the successful crystallization of **1**−**5**, as shown in Scheme 1. Thus, all compounds contained a Na^+- or K^+-18-crown-6-ether molecule as the countercation. In our previous work, only the compound with 5-Clsalpy^{2-} was isolated as a formulation of $Na(THF)_2[Ru_2(O_2CCH_3)_2(5\text{-Clsalpy})_2]$·THF without a bulky countercation such as Na^+-18-crown-6-ether.[7]

The magnetic data of metal−metal bonded diruthenium compounds have provided important information regarding the oxidation of ruthenium ions and the electronic configuration in the diruthenium frontier orbitals. The magnetic

Scheme 1

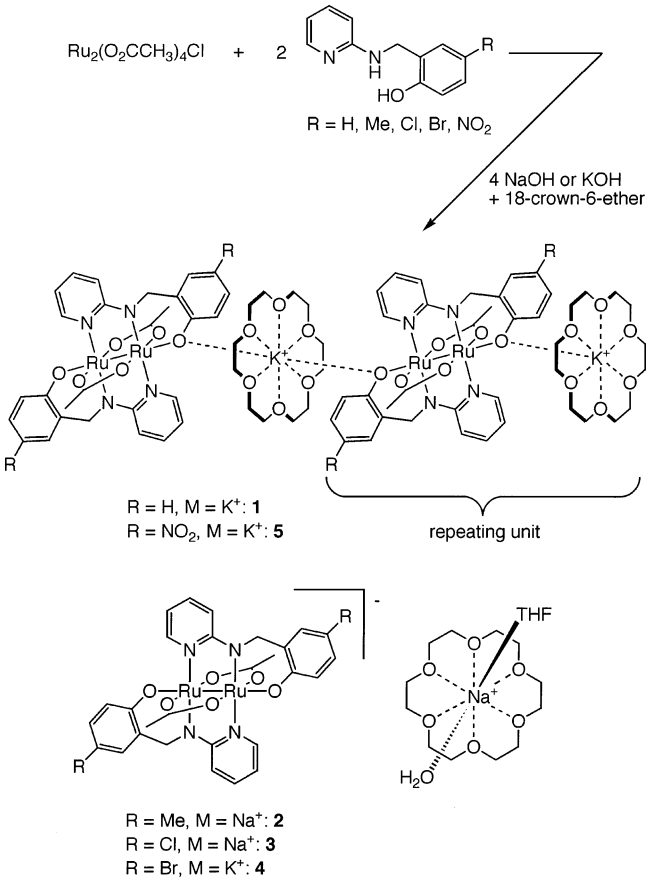

susceptibilities of **1**−**5** were therefore measured in the temperature range 1.8−300 K to confirm their electronic state in the solid state. The χT products at 300 K found in the range 1.82−1.89 cm^3·K·mol^{-1} were gradually decreased upon cooling to finally reach minimum values at 1.8 K (0.98−1.25 cm^3·K·mol^{-1}) (Figure S1). At low temperatures, a small kink was observed in **2**, **3**, and **4**, which may be due to contamination by a small amount of Ru_2(III,III) species that possess an $S = 1$ state and/or Ru(III) monomer species

(12) *Crystal Structure Analysis Package*; Molecular Structure Corporation: The Woodlands, TX, 1985 and 1992.
(13) Miyasaka, H.; Sugiura, K.; Yamashita, M. *Inorg. Chem. Commun.* **2003**, *6*, 1078.
(14) Miyasaka, H.; Chang, H.-C.; Mochizuki, K.; Kitagawa, S. *Inorg. Chem.* **2001**, *40*, 3544.

($S = {}^1/_2$). As the decrease of the χT product should be mainly due to a contribution of the zero-field splitting (ZFS), best-fitting simulation was performed using the $S = {}^3/_2$ paramagnetic Van Vleck equation with ZFS contribution (D).[15] The parameter sets estimated by a simulation above 10 K are the following: $g = 2.02$, $D = 56.8$ cm^{-1} ($R = 0.9986$) for **1**; $g = 1.98$, $D = 60.1$ cm^{-1} ($R = 0.9968$) for **2**; $g = 2.00$, $D = 53.2$ cm^{-1} ($R = 0.9921$) for **3**; $g = 2.02$, $D = 58.7$ cm^{-1} ($R = 0.9971$) for **4**; and $g = 2.01$, $D = 60.5$ cm^{-1} ($R = 0.9990$) for **5** ($R = 1 - \sum\{(\chi T_{calc} - \chi T_{obs})/\sum(\chi T_{obs})\}^2$). The obtained g values seem to be slightly small compared with those of the other Ru_2(II,III) compounds reported so far, thereby suggesting contamination by diamagnetic and paramagnetic species possessing a small spin state of $S = 1$ and/or $S = {}^1/_2$, as aforementioned.[15] The ZFS values are in good agreement with the previously reported values for the paddlewheel type diruthenium(II,III) compounds ($D \approx 40-80$ cm^{-1}).[16−24] These magnetic data agree with **1**−**5** consisting of a Ru_2^{5+} unit with an electronic configuration of $\sigma^2\pi^4\delta^2(\pi^*\delta^*)^3$.

Structures. The structural feature of the anionic part, $[Ru_2(O_2CCH_3)_2(R\text{-salpy})_2]^-$, is very similar among the compounds. The structures of **1** and **5** including the K^+-18-crown-6-ether molecule are shown in Figure 1. Because **2**, **3**, and **4** possess two kinds of anionic parts that are very similar to each other, only a representative one is depicted in Figure 2. The selected bond distances and angles for all compounds are summarized in Table 2. It should be mentioned that the R-salpy^{2-} ligand acts as a tridentate ligand having both bridging and chelating characters to form the M−M bridging/axial- or equatorial-chelating mode. The designed tridentate ligands contain amino-pyridyl and phenolate moieties connected by a methylene group, where the former can attach to the dimetal unit and the latter can flexibly cap the axial (M−M bridging/axial-chelating mode: Chart 1a) or equatorial position (M−M bridging/equatorial-chelating mode: Chart 1b). All the present compounds have the M−M bridging/axial-chelating mode. In addition, it should be noted that such equatorial ligands as $CH_3CO_2^-$ and R-salpy^{2-} are located around a diruthenium unit in a *trans* fashion.[5] The dimeric compounds with paddlewheel structures gave the *cis* conformation in the substitution reaction in many cases.[3,5,6] That the Ru−Ru bond distances are 2.300(1) Å for **1**; 2.2971(8), 2.2966(8) Å for **2**; 2.291(1), 2.285(1) Å for **3**; 2.2922(9), 2.289(1) Å for **4**; and 2.2833(8) Å for **5** are proof of their Ru_2^{5+} oxidation states with the electronic configuration $\sigma^2\pi^4\delta^2(\pi^*\delta^*)^3$ because of their similarity to the values observed in typical paddlewheel-type Ru_2^{5+} compounds (2.27−2.30 Å).[16,24] This conclusion is consistent with the aforementioned magnetic data. The amino-pyridyl moiety of the R-salpy^{2-} ligand bridges the diruthenium unit with average bond distances of $(Ru-N_{pyridine})_{av} = 2.078$ Å and $(Ru-N_{aminato})_{av} = 2.034$ Å, whereas the distances between Ru and carboxylate oxygen are found in the range 2.041−2.073 Å. Two phenolate moieties acting as pendant ligands cap the axial positions of the Ru−Ru bond with distances and angles of Ru(1)−O(1) = 2.222(6) Å and O(1)−Ru(1)−Ru(1)* = 175.6(2)° for **1**; Ru(1)−O(1) = 2.201(3) Å, Ru(2)−O(4) = 2.211(4) Å, and

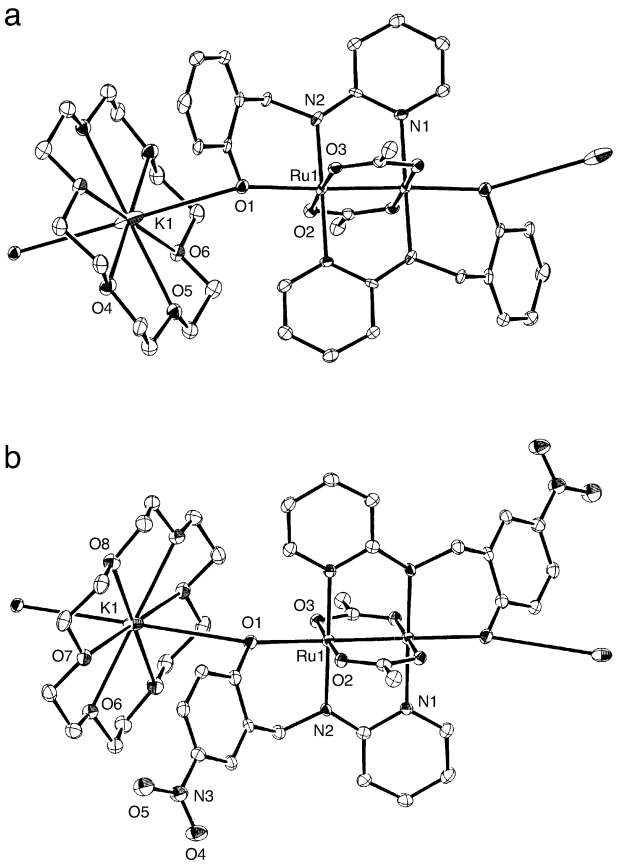

Figure 1. Structural drawings of an asymmetrical unit of **1** (a) and **5** (b).

(15) If the main contributor to the decrease of the magnetic moment is the ZFS effect, the following expressions for the magnetic susceptibility of $S = {}^3/_2$ are applicable (O'Connor, C. J. *Prog. Inorg. Chem.* **1982**, *29*, 203):

$$\chi_{||} = \frac{Ng^2\beta^2}{k_BT}\frac{1 + 9e^{-2x}}{4(1 + e^{-2x})} \quad (2)$$

$$\chi_{\perp} = \frac{Ng^2\beta^2}{k_BT}\frac{4 + \frac{3}{x}(1 - e^{-2x})}{4(1 + e^{-2x})} \quad (3)$$

where x is $D/(k_BT)$ and D is the magnitude of the ZFS. The average molar magnetic susceptibility is given as follows:

$$\chi = \frac{\chi_{||} + 2\chi_{\perp}}{3} \quad (4)$$

As mentioned in the text, some impurities such as Ru_2(III,III) species or Ru(III) monomer species are surmised to exist in the samples, particularly in **2**, **3**, and **4**. However, in this work, eq 4 was used for all compounds to simulate the susceptibility data above 10 K (Figure S1). In addition, the contributions of temperature-independent paramagnetism (TIP) and term of intermolecular interaction were excluded for simplicity, although those have been included in some cases of Ru_2(II,III) materials reported so far.

(16) Aquino, M. A. S. *Coord. Chem. Rev.* **1998**, *170*, 141.
(17) Jiménez-Aparicio, R.; Urbanos, F. A.; Arrieta, J. M. *Inorg. Chem.* **2001**, *40*, 613.
(18) Beck, E. J.; Drysdale, K. D.; Thompson, L. K.; Li, L.; Murphy, C. A.; Aquino, M. A. S. *Inorg. Chim. Acta* **1998**, *279*, 121.
(19) Barral, M. C.; Jiménez-Aparicio, R.; Pérez-Quintanilla, D.; Priego, J. L.; Royer, E. C.; Torres, M. R.; Urbanos, F. A. *Inorg. Chem.* **2000**, *39*, 65.
(20) Cukiernik, F. D.; Giroud-Godquin, A.-M.; Maldivi, P.; Marchon, J.-C. *Inorg. Chim. Acta* **1994**, *215*, 203.
(21) Telser, J.; Drago, R. S. *Inorg. Chem.* **1984**, *23*, 3114.
(22) Cukiernik, F. D.; Luneau, D.; Marchon, J.-C.; Maldivi, P. *Inorg. Chem.* **1998**, *37*, 3698.
(23) Miyasaka, H.; Clérac, R.; Campos-Fernández, C. S.; Dunbar, K. R. *Inorg. Chem.* **2001**, *40*, 1663.
(24) Cotton, F. A.; Walton, R. A. *Multiple Bonds between Metal Atoms*, 2nd ed.; Oxford University Press: Oxford, 1993.

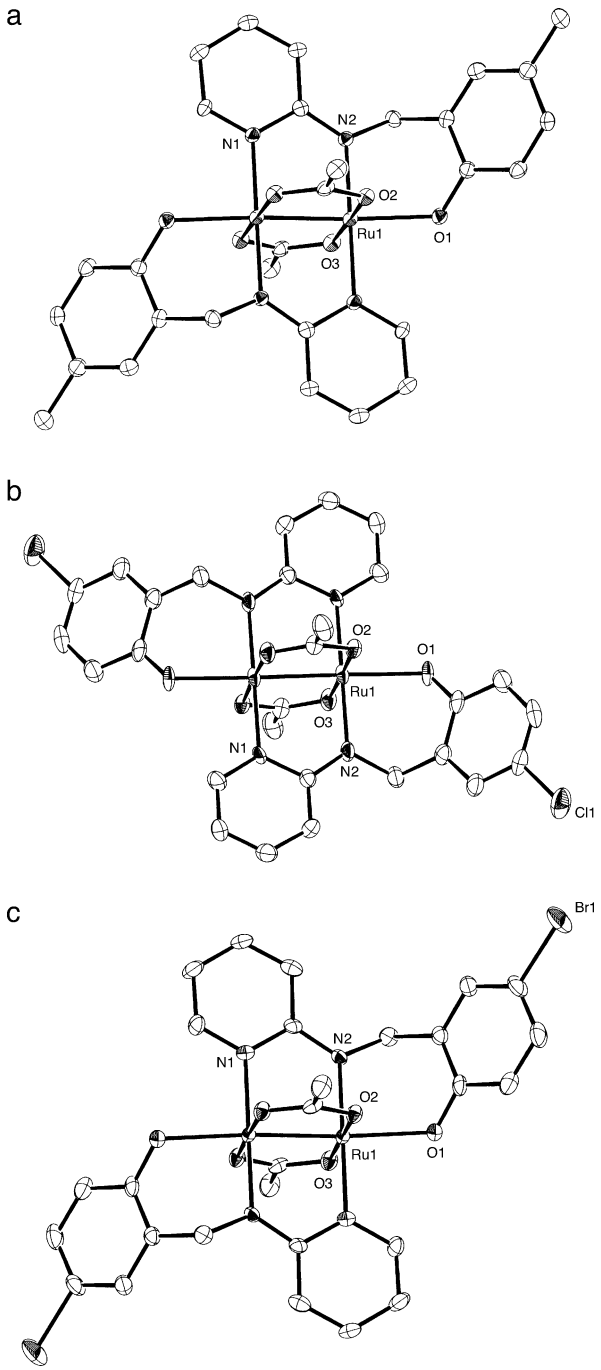

Figure 2. Structural drawings of an anionic unit of **2** (a), **3** (b), and **4** (c).

O(1)−Ru(1)−Ru(1)* = 176.40(9)°, O(4)−Ru(2)−Ru(2)* = 176.1(1)° for **2**; Ru(1)−O(1) = 2.209(5) Å, Ru(2)−O(4) = 2.205(5) Å, and O(1)−Ru(1)−Ru(1)* = 175.3(1)°, O(4)−Ru(2)−Ru(2)* = 176.2(1)° for **3**; Ru(1)−O(1) = 2.212(4) Å, Ru(2)−O(4) = 2.207(4) Å, and O(1)−Ru(1)−Ru(1)* = 174.6(1)°, O(4)−Ru(2)−Ru(2)* = 176.4(1)° for **4**; and Ru(1)−O(1) = 2.223(4) Å and O(1)−Ru(1)−Ru(1)* = 177.88(9)° for **5**. Note that these structural features of the Ru−Ru core were likewise observed in $Na(THF)_2[Ru_2(O_2CCH_3)_2(5\text{-Clsalpy})_2]\cdot THF$ reported previously.

In **1** and **5** with the K^+(18-crown-6) countercation, the phenolate oxygen of R-salpy^{2-} interacts with K^+ with bond distances of 3.289(6) Å for **1** and 3.359(3) Å for **5** to form an alternating one-dimensional (1-D) arrangement of repeating [···K···O−Ru−Ru−O···] units, as shown in Figure 3. In contrast, **2**, **3**, and **4** with the Na^+(18-crown-6) countercation exist as discrete species (Figure 2). The one-dimensional arrangement consisting of the alkaline metal ion and Ru_2 unit was also found in $Na(THF)_2[Ru_2(O_2CCH_3)_2(5\text{-Clsalpy})_2]\cdot THF$, in which the Na ion was surrounded by two phenolate oxygens, two acetate oxygens, and two THF molecules to form an alternating 1-D chain with a repeating unit of $[\cdots Na(THF)_2\cdots(O_{PhO/AcO})_2-Ru-Ru-(O_{PhO/AcO})_2\cdots]$.[7]

Table 2. Relevant Bond Distances (Å) and Angles (deg) of **1**−**5** with Estimated Standard Deviations in Parentheses

	1·THF	**2**·0.5THF	**3**·0.5THF	**4**·0.5THF	**5**·2THF
		Distances (Å)			
Ru(1)−Ru(1)*[a]	2.300(1)	2.2971(8)	2.291(1)	2.2922(9)	2.2833(8)
Ru(1)−O(1)	2.222(6)	2.201(3)	2.209(5)	2.212(4)	2.223(4)
Ru(1)−O(2)	2.041(5)	2.071(4)	2.073(5)	2.057(4)	2.064(3)
Ru(1)−O(3)	2.057(5)	2.061(4)	2.056(5)	2.055(4)	2.049(3)
Ru(1)−N(1)*	2.085(6)	2.071(4)	2.093(6)	2.073(4)	2.079(3)
Ru(1)−N(2)	2.027(6)	2.033(4)	2.037(6)	2.031(4)	2.033(3)
Ru(2)−Ru(2)**[b]		2.2966(8)	2.285(1)	2.289(1)	
Ru(2)−O(4)		2.211(4)	2.205(5)	2.207(4)	
Ru(2)−O(5)		2.061(4)	2.048(5)	2.047(4)	
Ru(2)−O(6)		2.066(4)	2.066(5)	2.064(4)	
Ru(2)−N(3)**		2.074(4)	2.080(6)	2.066(5)	
Ru(2)−N(4)		2.036(4)	2.035(6)	2.036(5)	
		Angles (deg)			
Ru(1)*−Ru(1)−O(1)	175.6(2)	176.40(9)	175.3(1)	174.6(1)	177.88(9)
Ru(1)*−Ru(1)−O(2)	90.2(2)	89.19(10)	89.1(1)	88.9(1)	89.18(9)
Ru(1)*−Ru(1)−O(3)	88.4(2)	89.1(1)	89.5(1)	89.8(1)	89.62(10)
Ru(1)*−Ru(1)−N(1)*	90.2(2)	90.8(1)	91.2(2)	91.0(1)	90.0(1)
Ru(1)*−Ru(1)−N(2)	90.0(2)	89.3(1)	89.3(2)	89.3(1)	90.6(1)
O(1)−Ru(1)−O(2)	94.0(2)	88.0(1)	86.9(2)	86.4(2)	92.9(1)
O(1)−Ru(1)−O(3)	87.5(2)	93.7(1)	94.6(2)	95.0(2)	88.3(1)
O(1)−Ru(1)−N(1)	91.1(2)	91.5(1)	91.2(2)	91.5(2)	90.3(1)
O(1)−Ru(1)−N(2)	88.8(2)	88.5(1)	88.3(2)	88.4(2)	89.0(1)
O(2)−Ru(1)−O(3)	178.4(2)	178.0(1)	178.2(2)	178.4(2)	178.8(1)
O(2)−Ru(1)−N(1)*	90.8(2)	90.3(2)	90.0(2)	91.1(2)	88.9(1)
O(2)−Ru(1)−N(2)	87.6(2)	91.6(2)	92.1(2)	91.6(2)	90.4(1)
O(3)−Ru(1)−N(1)*	88.5(2)	88.7(2)	88.9(2)	88.0(2)	91.0(1)
O(3)−Ru(1)−N(2)	93.1(2)	89.4(2)	88.9(2)	89.4(2)	89.8(1)
N(1)*−Ru(1)−N(2)	178.4(2)	178.1(2)	177.8(2)	177.3(2)	179.0(2)
Ru(2)**−Ru(2)−O(4)		176.1(1)	176.2(1)	176.4(1)	
Ru(2)**−Ru(2)−O(5)		90.1(1)	90.1(2)	90.3(1)	
Ru(2)**−Ru(2)−O(6)		88.3(1)	88.5(1)	88.3(1)	
Ru(2)**−Ru(2)−N(3)		89.8(1)	89.4(2)	89.6(1)	
Ru(2)**−Ru(2)−N(4)		90.5(1)	91.1(2)	91.0(1)	
O(4)−Ru(2)−O(5)		93.7(1)	93.5(2)	93.1(2)	
O(4)−Ru(2)−O(6)		87.9(1)	88.0(2)	88.3(2)	
O(4)−Ru(2)−N(3)**		91.3(2)	92.0(2)	91.6(2)	
O(4)−Ru(2)−N(4)		88.5(2)	87.6(2)	87.9(2)	
O(5)−Ru(2)−O(6)		178.1(1)	178.4(2)	178.6(2)	
O(5)−Ru(2)−N(3)**		88.1(2)	88.8(2)	88.5(2)	
O(5)−Ru(2)−N(4)		89.3(2)	88.9(2)	88.7(2)	
O(6)−Ru(2)−N(3)**		90.9(2)	90.5(2)	90.9(2)	
O(6)−Ru(2)−N(4)		91.8(2)	91.8(2)	91.9(2)	
N(3)**−Ru(2)−N(4)		177.4(2)	177.6(2)	177.1(2)	

[a] Symmetry operations (*): $-x, -y, -z+2$ for **1**; $-x, -y+1, -z$ for **2**; $-x, -y, -z$ for **3**; $-x, -y+1, -z$ for **4**; and $-x, -y, -z$ for **5**. [b] Symmetry operations (**): $-x, -y, -z$ for **2**; $-x, -y+1, -z$ for **3**; and $-x, -y, -z$ for **4**.

Chart 1

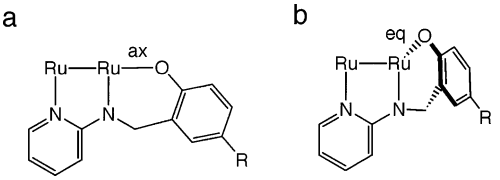

Electrochemistry. The electronic behavior of **1**−**5** was confirmed by cyclic voltammetry (CV) and differential pulse voltammetry (DPV) in MeCN containing *n*-$Bu_4N(BF_4)$ as

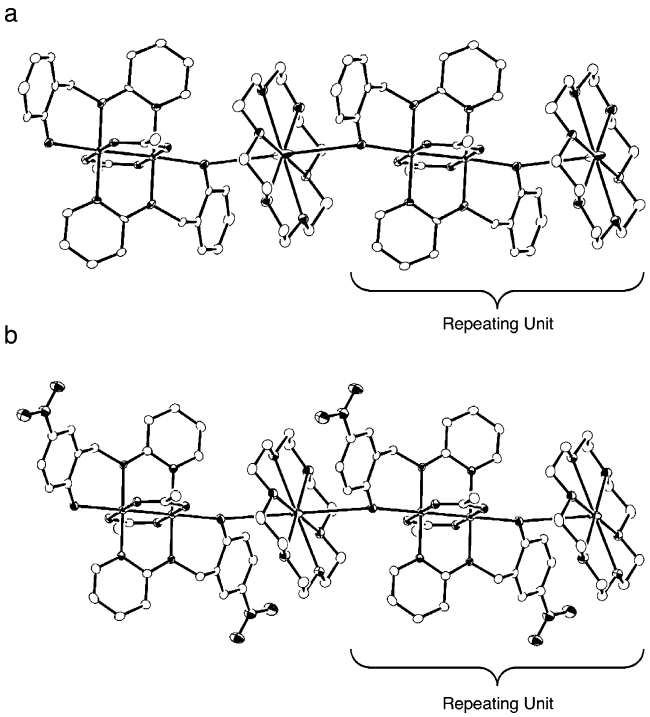

Figure 3. 1-D chain structures of **1** (a) and **5** (b).

the supporting electrolyte (vs Ag/AgCl). The data for all the compounds revealed rich redox chemistry and basically identical redox processes: one reduction and three oxidations were found as waves A−D, as shown in Figure 4. The additional waves E−G are related to subspecies that were newly produced during electrochemical measurements (vide infra). The observed redox potentials for all compounds are summarized in Table 3. Note that the electrochemical behavior of **3** is essentially identical to that of $Na(THF)_2$-$[Ru_2(O_2CCH_3)_2(5\text{-Clsalpy})_2]\cdot THF$.[7] The one-electron reduction (couple A in Figure 4) is assigned to Ru_2^{5+}/Ru_2^{4+} (r) and is observed in the $E_{1/2}$ potential range −1.51 to −1.27 V. For the oxidation process, the first and second couples (couples B and C in Figure 4, respectively) are assigned to the metal-centered ones, Ru_2^{6+}/Ru_2^{5+} (r) and Ru_2^{7+}/Ru_2^{6+} (qr or ir), and are observed in the $E_{1/2}$ potential ranges −0.38 to −0.03 V and 0.22 to 0.39 V, respectively. Thus, the observation of relative lower oxidation potentials is attributed to the strong donor nature of the dianionic ligands R-salpy^{2-}, although 5-Clsalpy^{2-}, 5-Brsalpy^{2-}, and 5-NO_2salpy^{2-} contain electron-withdrawing substituents. Such ligands consequently stabilize the high oxidation state of Ru_2^{6+} and Ru_2^{7+}. The third couple (D in Figure 4) observed in the $E_{1/2}$ potential range 0.81−1.08 V may be accomplished by two-electron oxidation arising from R-salpy^{2-}-centered oxidations (ir). This assignment may be supported by what the CV data of R-salpyH_2 in MeCN reveal to be an irreversible one-electron oxidation at $E_{1/2}$ higher than 0.5 V. The ambiguous peak separation in the R-salpy^{2-} oxidation, even in **2** that gives two peaks in DPV (see Table 3), suggests incomplete electronic communication between R-salpy^{2-} ligands via the Ru_2^{7+} unit.[25] Although oxidations of Ru_2^{6+}, forming Ru_2^{7+}, and R-salpy^{2-} ligand are actually observed, albeit irreversibly, these oxidation processes would make it difficult for the complex to remain in the complete form in solution.

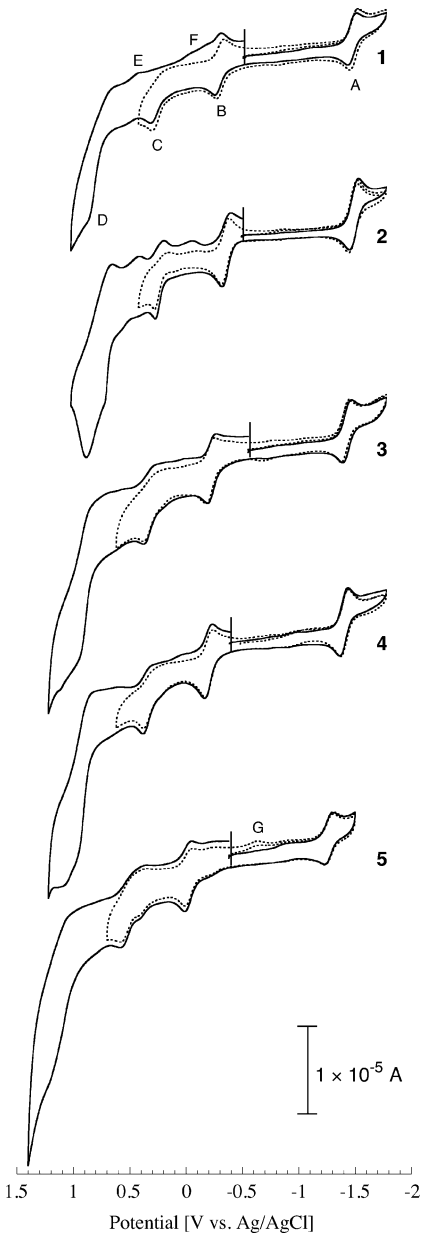

Figure 4. Cyclic voltammograms of **1**−**5** in MeCN containing 0.2 M TBA-(BF_4) under N_2.

Indeed, repeated CV cycles led to the appearance of new waves E−G in Figure 4 in the backward sweep (cathodic peaks). These additional waves are observed when the potential is swept over ligand redox range (∼1.4 V) and are probably due to modified forms such as ligand-"partially"-free species, as shown in Scheme 2.

The redox potentials of **1**−**5** are strongly dependent on the electronic character of the R-substituent. Interestingly, the respective redox potentials exhibit a linear correlation with the Hammett substituent constant σ_p.[26] Figure 5 shows a plot of $E_{1/2}$ versus $2\sigma_p$, where 2 is the number of substituents per compound. Here, the linear least-squares fit

(25) On CVs, no peak separation related to oxidations based on two R-salpy^{2-} ligands was detectable, but on a DPV, a broad peak that contained two 1e$^-$ oxidations was observed for **1** and **3**−**5**. For **2**, a slight peak separation was observed (peak-to-peak separation Δ_p = 135 mV).

Table 3. Electrochemical Data of **1**−**5** Measured in MeCN Containing 0.2 M TBA(BF_4) under N_2 (V vs Ag/AgCl)[a]

compd	Hammett constant[b]	A Ru_2^{5+}/Ru_2^{4+}	B Ru_2^{6+}/Ru_2^{5+}	C Ru_2^{7+}/Ru_2^{6+}	D1 L/L^-	D2 L/L^-
1	0	−1.511[c]	−0.326[c]	0.281[e]	0.867[e]	
		(−1.490)[d]	(−0.316)[d]	(0.252)[d]	(0.810)[d]	
2	−0.17	−1.504[c]	−0.371[c]	0.259[e]	0.704[e]	0.864[e]
		(−1.506)[d]	(−0.381)[d]	(0.220)[d]	(0.675)[d]	(0.810)[d]
3	0.23	−1.446[c]	−0.238[c]	0.355[e]	0.982[e]	
		(−1.440)[d]	(−0.254)[d]	(0.312)[d]	(0.886)[d]	
4	0.23	−1.427[c]	−0.227[c]	0.361[e]	0.977[e]	
		(−1.417)[d]	(−0.218)[d]	(0.330)[d]	(0.908)[d]	
5	0.78	−1.282[c]	−0.029[c]	0.585[e]	1.205[e]	
		(−1.274)[d]	(−0.029)[d]	(0.394)[d]	(1.082)[d]	

[a] The ferrocene/ferrocenium couple, $Fc/Fc^+ = 0.08$ V ($I_c/I_a \approx 1$, $\Delta E_p =$ 75 mV), was observed at the same condition described in the Experimental Section in the text. [b] Reference 25. [c] Half-wave potentials ($E_{1/2}$'s) from cyclic voltammograms. The couples of A and B were estimated because of their reversibility ($I_c/I_a \approx 1$, $\Delta E_p \approx 74$ mV at a scan rate of 0.03 V/ s). [d] Peak potentials from differential pulse voltammograms (scan rate, 8 mV/ s; pulse width, 60 ms; pulse period, 120 ms). [e] Anode peaks because of their irreversibility.

Scheme 2

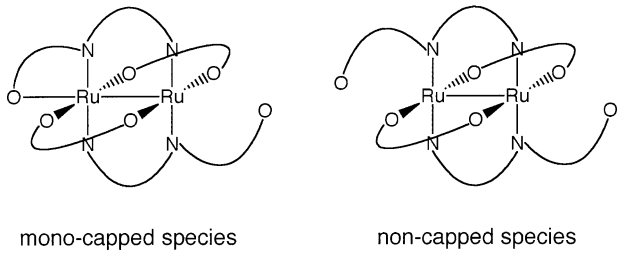

gives a correlation in the form of eq 1:

$$\Delta E_{1/2} = E_{1/2}(\mathrm{X}) - E_{1/2}(\mathrm{H}) = 2\sigma_p\rho \qquad (1)$$

From this correlation, the reactivity constants ρ for the redox processes are 127 mV for Ru_2^{5+}/Ru_2^{4+}, 185 mV for Ru_2^{6+}/Ru_2^{5+}, 92 mV for Ru_2^{7+}/Ru_2^{6+}, and 179 mV for R-salpy$^{\bullet -}$/R-salpy^{2-}, which are very similar to each other and comparable to the value observed for the ionization of R-salpyH_2 ($\rho = 171$ mV). The similarity in ρ between metal-centered redox and ligand-centered redox leads us to the understanding that the diruthenium unit is significantly influenced by the substituents via phenolate and benzylaminate subgroups, where the former way may be dominant because of the existence of a methylene spacer in the latter. Further, the result indicates the ability of the 5-substituent, i.e., the R group of R-salpy^{2-} ligands, to tune the redox potentials of the diruthenium unit. Some studies on the linear free energy relationships in M−M bonded dinuclear compounds have been reported.[27] The ρ values obtained in our study are larger than those derived from dimetal-centered redoxes on [M_2-(di-R-arylformamidinate)$_4$] (M = Mo, Ni, and Ru): for example, Ren et al. showed the possibility of electronic and spectroscopic tuning of the corresponding Ru_2(II,III) complexes by the R-substituents on di-R-arylformamidinate and

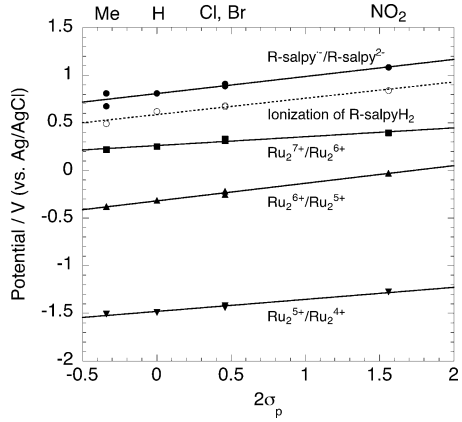

Figure 5. Hammett plot of redox potentials (vs Ag/AgCl in MeCN with 0.2 M TBA(BF_4)): H, **1**; Me, **2**; Cl, **3**; Br, **4**; NO_2, **5**. For the referred potentials, the peak potentials in differential pulse voltammograms are used (see Table 3).

Table 4. UV−Vis−NIR Spectral Data of **1**−**5** in MeCN under N_2

	λ_{max}, nm ($\epsilon/10^3 \cdot M^{-1} \cdot cm^{-1}$)				
compd	band I	band II	band III	band IV	band V
1		430 (sh)	581 (2.8)	680 (sh)	1046 (0.8)
2	308 (22)	442 (5.6)	582 (5.1)	680 (sh)	1045 (1.3)
3	312 (sh)	438 (5.2)	585 (5.1)	670 (sh)	1046 (1.6)
4	290 (sh)	437 (5.3)	584 (4.4)	670 (sh)	1051 (1.3)
5			580 (sh)	640 (sh)	1030 (0.7)

revealed reactivity constants $\rho = 69.3$ mV and 88.9 mV for $Ru_2^{II,III}/Ru_2^{II,II}$ and $Ru_2^{III,III}/Ru_2^{II,III}$ redoxes, respectively.[28] Recently, Kadish et al. reported a substituent effect on the electrochemistry and spectrochemistry of Ru_2(II,III) complexes containing four identical unsymmetrical bridging ligands, 2-(R-anilino)pyridinate anion, where R = H, 2-CH_3, 2-F, 2,5-F_2, 2,6-F_2, 2,4,6-F_3, or F_5.[29] In those compounds, the substituents on the anilino group and the conformation of the ligands around the diruthenium unit systematically affected their redox behaviors, obeying the Hammett relationship, and the HOMO−LUMO gap between π^* and δ^* energy levels on the electronic ground state of $\sigma^2\pi^4\delta^2\pi^{*2}$ for the singly oxidized compounds (Ru_2^{6+}). The reaction constants (ρ) for the metal-centered redox in our compounds are slightly larger than the values reported in these studies.

UV−Vis−NIR Spectra. The absorption spectra of the MeCN solutions of **1**−**5** were measured in the range 280−1200 nm (UV−vis−NIR region): the data are summarized in Table 4. Except **5**, all compounds exhibited three characteristic bands labeled as II, III, and V with a shoulder band IV in the visible region (Figure 6 for **3**). The wavelengths for observing these absorption bands are, respectively, very similar among the series of the compounds regardless of their substituents: 430−442 nm for II, 581−587 nm for III, 670−680 nm for IV, and 1045−1051 nm for V in **1**−**4**. Bands III and IV are understandable, because

(26) (a) Hammett, L. P. *J. Am. Chem. Soc.* **1937**, *59*, 96. (b) van Bekkum, H.; Verkade, P. E.; Wepster, B. M. *Recl. Trav. Chim. Pays-Bas* **1959**, *78*, 815. (c) Exner, O. *Correlation Analysis of Chemical Data*; Plenum: New York, 1988. (d) Hafe, H. H. *Chem. Rev.* **1953**, *53*, 191. (e) Zuman, P. *The Elucidation of Organic Electrode Processes*; Academic Press: New York, 1969.

(27) (a) Lin, C.; Protasiewicz, J. D.; Smith, E. T.; Ren, T. *J. Chem. Soc., Chem. Commun.* **1995**, 2257. (b) Lin, C.; Protasiewicz, J. D.; Smith, E. T.; Ren, T. *Inorg. Chem.* **1996**, *35*, 6422. (c) Lin, C.; Protasiewicz, J. D.; Ren, T. *Inorg. Chem.* **1996**, *35*, 7455. (d) Carlson-Day, K. M.; Eglin, J. L.; Lin, C.; Smith, L. T.; Staples, R. J.; Wipf, O. *Polyhedron* **1999**, 817.

(28) Lin, C.; Ren, T.; Valente, E. J.; Zubkowski, J. D.; Smith, E. T. *Chem. Lett.* **1997**, 753.

(29) Kadish, K. M.; Wang, L.-L.; Thuriere, A.; Caemelbecke, E. V.; Bear, J. L. *Inorg. Chem.* **2003**, *42*, 834.

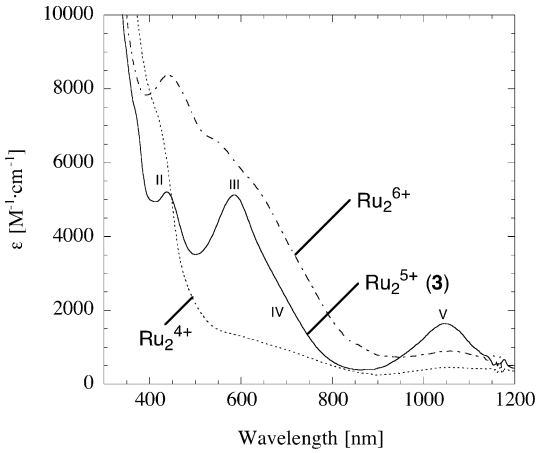

Figure 6. UV−vis−NIR spectra of **3**, singly reduced species, and singly oxidized species in MeCN, where the latter two species were generated by using a bulk electrochemical cell with 0.2 M TBA(BF_4).

Table 5. UV−Vis−NIR Spectral Data of Singly Reduced Species (Ru_2^{4+}) and Singly Oxidized Species (Ru_2^{6+}) of **3**

oxidation state	λ_{max}, nm ($\epsilon/10^3$·M^{-1}·cm^{-1})			
	band II	band III	band IV	band V
Ru_2^{6+}	441 (8.4)	548 (sh)	628 (sh)	1059 (0.9, br)
Ru_2^{5+} (**3**)	438 (5.2)	584 (5.1)	670 (sh)	1046 (1.6)
Ru_2^{4+}	412 (sh)	620 (sh)		1058 (0.5, br)

of the dark green color of the compounds. In **5**, bands III and V are clearly observed at 580 and 1030 nm, respectively; band III is broad because it overlaps with band IV at approximately 640 nm. It is noteworthy that the overall spectral features of these compounds are similar to those of a mono-(*N*,*N*-ligand)-substituted compound, $[Ru_2(O_2CCH_3)_3$(admpym)(Cl)(MeOH)] (Hadmpym = 2-amino-4,6-dimethylpyrimidine),[30] or a di-(*O*,*N*-ligand)-substituted compound, $Ru_2(O_2CCH_3)_2(mhp)_2Cl$ (mhp^- = 6-methyl-2-pyridonate),[31] or a tetra-(*O*,*N*-ligand) compound, $Ru_2(chp)_4Cl$ (chp^- = 6-chloro-2-pyridonate).[32]

For **3**, the singly oxidized Ru_2^{6+} species and the singly reduced Ru_2^{4+} species were generated by bulk controlled-potential electrolyses in MeCN containing 0.2 M TBA(BF_4) at potentials slightly more positive than $E_{1/2}^{((1-e)ox)}$ and slightly more negative than $E_{1/2}^{((1-e)red)}$. Each of the generated species was monitored by spectroscopy, as shown in Figure 6, and the data are summarized in Table 5. The spectrum of the singly oxidized species (Ru_2^{6+} in Figure 6) exhibited three intense bands at 440 nm (ϵ = 8300 M^{-1}·cm^{-1}), 548 nm (sh), and 628 nm (sh). The band around 1000 nm observed in the original compound **3** almost disappeared in the spectrum of the singly oxidized species. Bands III and IV were slightly shifted to shorter wavelengths than those of **3**, and indeed, the solution color became dark (purplish brown) compared to the green color of **3**. On the other hand, the spectrum of the singly reduced Ru_2^{4+} species exhibited not intense absorption peaks but some shoulder bands at 412 and 620 nm (the solution color is pale brown). All compounds were also slowly oxidized under aerobic conditions: the spectral variation during air oxidation of **3** was monitored (Figure S2). The initial spectrum of **3** was gradually varied, and after 40 h, the spectrum of a singly oxidized species was observed, indicating complete oxidation. Thus, the observed spectrum is almost the same as that produced by bulk controlled-potential electrolyses, namely, the final spectrum assigned to Ru_2^{6+} species.

Summary

A series of $[A(18\text{-crown-6})(S)_x][Ru_2(O_2CCH_3)_2(R\text{-salpy})_2]$ compounds (R = H, **1**; Me, **2**; Cl, **3**; Br, **4**; NO_2, **5**) were isolated using the Na^+- or K^+-18-crown-6-ether complex as the countercation. Compounds **1** and **5** containing the K^+-18-crown-6-ether were characterized by novel one-dimensional chain structures of repeating [···K···O−Ru−Ru−O···] units. In our previous work, we were able to isolate only $[Ru_2(O_2CCH_3)_2(5\text{-Cl-salpy})_2]^-$ with the Na^+ cation.[7] In this work, the use of Na^+- or K^+-18-crown-6-ether cation let to successful isolation and characterization of these species. Systematic redox activities obeying the Hammett law based on the Ru_2 center and the substituted ligand were observed in their electrochemistry. Couples containing the single reduction and the first single oxidation on the Ru_2 center were reversible, whereas the couple with the second oxidation to form Ru_2^{7+} was almost irreversible. Nevertheless, all the metal-centered redox processes occurred at lower potentials than those of general paddlewheel-type Ru_2^{5+} complexes, $Ru_2(O_2CR)_4^+$.[16] The singly oxidized and reduced species of **3** were generated by bulk controlled-potential electrolyses and monitored by spectroscopy. The ligand-centered oxidation occurred at potentials higher than 0.7 V (vs Ag/AgCl), but it is irreversible and is assigned as a two-electron oxidation process in almost all compounds. As mentioned in the Introduction, d−π conjugated systems containing redox-active ligands that fully electrically couple between them via the metal−metal bonding unit are our targets. In **2,** having 5-$Mesalpy^{2-}$ that contains an electron-donating substituent, at least two single redox couples were observed in the potential range 0.7−0.9 V (see Table 3). The observation of two redox couples at such high potentials may be an indication of the existence of electronic interaction via the Ru_2^{7+} unit. Investigations using the series ligand derivatives containing electron-donating substituents are underway to clarify such ligand-to-ligand electronic interactions in our system.

Supporting Information Available: X-ray crystallographic files in CIF format for the structure determination of **1**−**5**, Figure S1 (χT vs T plots for all compounds), and Figure S2 (spectral variation by air oxidation of **3**). This material is available free of charge via the Internet at http://pubs.acs.org.

IC034625K

(30) Kachi-Terajima, C.; Miyasaka, H.; Ishii, T.; Sugiura, K.; Yamashita, M. *Inorg. Chim. Acta* **2002**, *332*, 210.
(31) Chakravarty, A. R.; Cotton, F. A.; Tocher, D. A. *Inorg. Chem.* **1985**, *24* (4), 2857.
(32) Chakravarty, A. R.; Cotton, F. A.; Tocher, D. A. *Inorg. Chem.* **1985**, *24*, 1263.